Food Microbiology 102 (2022) 103915

Contents lists available at ScienceDirect

Food Microbiology

journal homepage: www.elsevier.com/locate/fm

Associations between *Listeria monocytogenes* genomic characteristics and adhesion to polystyrene at 8 °C

David Burke James Mahoney [a], Justin Falardeau [a], Patricia Hingston [a], Cora Chmielowska [b], Laura M. Carroll [c], Martin Wiedmann [c], Sung Sik Jang [d], Siyun Wang [a,*]

[a] Department of Food, Nutrition, and Health, University of British Columbia, Vancouver, BC, Canada
[b] Department of Bacterial Genetics, University of Warsaw, Warsaw, Poland
[c] Department of Food Science, Cornell University, Ithaca, NY, USA
[d] British Columbia Centre for Disease Control, Vancouver, BC, Canada

ARTICLE INFO

Keywords:
Listeria monocytogenes
Internalin A
Stress survival islet 1
Adhesion
Clonal complex
Genome wide association study

ABSTRACT

Listeria monocytogenes remains a threat to the food system and has led to numerous foodborne outbreaks worldwide. *L. monocytogenes* can establish itself in food production facilities by adhering to surfaces, resulting in increased resistance to environmental stressors. The aim of this study was to evaluate the adhesion ability of *L. monocytogenes* at 8 °C and to analyse associations between the observed phenotypes and genetic factors such as internalin A (*inlA*) genotypes, stress survival islet 1 (SSI-1) genotype, and clonal complex (CC). *L. monocytogenes* isolates (n = 184) were grown at 8 °C and 100% relative humidity for 15 days. The growth was measured by optical density at 600 nm every 24 h. Adherent cells were stained using crystal violet and quantified spectrophotometrically. Genotyping of *inlA* and SSI-1, multi-locus sequence typing, and a genome-wide association study (GWAS) were performed to elucidate the phenotype-genotype relationships in *L. monocytogenes* cold adhesion. Among all *inlA* genotypes, truncated *inlA* isolates had the highest mean adhered cells, ABS595nm = 0.30 ± 0.15 (Tukey HSD; $P < 0.05$), while three-codon deletion *inlA* isolates had the least mean adhered cells (Tukey HSD; $P < 0.05$). When SSI-1 was present, more cells adhered; less cells adhered when SSI-1 was absent (Welch's *t*-test; $P < 0.05$). Adhesion was associated with clonal complexes which have low clinical frequency, while reduced adhesion was associated with clonal complexes which have high frequency. The results of this study support that premature stop codons in the virulence gene *inlA* are associated with increased cold adhesion and that an invasion enhancing deletion in *inlA* is associated with decreased cold adhesion. This study also provides evidence to suggest that there is an evolutionary trade off between virulence and adhesion in *L. monocytogenes*. These results provide a greater understanding of *L. monocytogenes* adhesion which will aid in the development of strategies to reduce *L. monocytogenes* in the food system.

1. Introduction

Listeria monocytogenes remains a threat to the food system by contaminating and persisting in food production facilities, leading to numerous outbreaks worldwide. This includes outbreaks in ready-to-eat deli meats in Canada and South Africa, which resulted in numerous fatalities and serious economic losses (Smith et al., 2019; Todd and Notermans, 2011). *L. monocytogenes* can persist in food production environments in part due to the ability to adhere to surfaces, which may lead to biofilm formation (Harrand et al., 2020). This adhesion phenotype is heterogeneous among *L. monocytogenes* strains; however, the exact mechanisms behind why some isolates adhere more than others remain unclear (Keeney et al., 2018).

Some associations with adhesion and the membrane-bound virulence protein, internalin A (*inlA*), have been previously identified (Franciosa et al., 2009; Keeney et al., 2018; Wang et al., 2015). Nevertheless, this phenotype-genotype relationship remains ambiguous. There are four identified genotypes of *inlA*: full length *inlA*, truncated *inlA*, three codon deletion (3CD) *inlA*, and *inlA* with a premature stop codon at position 9 (9aa PMSC *inlA*) (Keeney et al., 2018; Kovacevic et al., 2013; Ragon et al., 2008). Full length *inlA* is the ancestral genotype containing a signal peptide, α-domain, leucine rich repeats, Ig-like

* Corresponding author.
E-mail address: siyun.wang@ubc.ca (S. Wang).

https://doi.org/10.1016/j.fm.2021.103915
Received 30 June 2021; Received in revised form 12 August 2021; Accepted 22 September 2021
Available online 23 September 2021

region, B-repeats, a pre-anchor, and a cell wall anchor (Lecuit et al., 1997; Ragon et al., 2008). The truncated *inlA* genotype is due to premature stop codons (PMSCs), which can occur from positions 462–700 within the B repeats region; these truncations remove the cell wall anchor, allowing the active site of the protein to be secreted (Franciosa et al., 2009). The 3CD *inlA* genotype is the result of the deletion of three amino acids, from positions 738–740, in the pre anchor (Kovacevic et al., 2013). Finally, the 9aa PMSC *inlA* genotype is due to a PMSC at the ninth amino acid, likely resulting in the failure to translate *inlA* (Keeney et al., 2018).

The relationship between strains with these *inlA* genotypes and adhesion has been examined, but the conclusions of these studies show a lack of consensus, plausibly because not all *inlA* genotypes were considered comprehensively. Furthermore, these studies were often conducted at higher temperatures, instead of in a cold environment where *L. monocytogenes* adhesion poses the greatest risk to the food industry; the following studies have conflicting results. In the first study, strains with a truncated *inlA* adhered more strongly than strains with a full length *inlA* (Franciosa et al., 2009). In the second study, strains with truncated *inlA* adhered equally to strains with a full length *inlA* (Keeney et al., 2018). In the final study, strains with a truncated *inlA* were not found in environments where adhesion would be advantageous (Wang et al., 2015). These results do not reach a consensus, leaving the association between *inlA* and adhesion unclear. Additionally, these *inlA* genotypes have been found to be causally associated with virulence phenotypes. Truncation of *inlA* leads to reduced internalization of *L. monocytogenes* into intestinal epithelial cells, resulting in reduced virulence, while the 3CD *inlA* leads to increased invasion ability of Caco-2 cells, which may lead to increased virulence (Jacquet et al., 2004; Kovacevic et al., 2013). The importance of *inlA* genotype is clear, which is why a comprehensive investigation into the association of all *inlA* genotypes and adhesion at a food industry-relevant temperature is needed.

Another genetic locus that has been shown to associate with *L. monocytogenes* adhesion is stress survival islet – 1 (SSI-1). SSI-1 is a five-gene operon, hypothesized to have integrated into the genome via transduction; SSI-1 has been reported to confer increased growth in acidic, saline, and food matrix environments (Ryan et al., 2010). Since previous investigations into the association between SSI-1 and adhesion were conducted at 30 °C, an investigation into the association of SSI-1 with adhesion at a food industry-relevant temperature is still necessary (Keeney et al., 2018).

The investigation of associations with single genetic variables, such as *inlA* and SSI-1, can be flawed, as these observations are confounded by the rest of the genome, which could also play a role in the phenotype being investigated, leading to a spurious association. One way to mitigate this issue is to examine the association of a phenotype with *L. monocytogenes* clonal complexes (CC). Clonal complexes are groups of sequence types, identified through multi-locus sequence typing (MLST), which categorize *L. monocytogenes* strains into evolutionarily distinct groups (Ragon et al., 2008). From the L. *monocytogenes* collection used in this study, two groups of clonal complexes were analysed: group A consisted of CC1, CC2, CC4, and CC6, while group B consisted of CC9 and CC121. Group A clonal complexes were chosen because they have been identified epidemiologically as being the most frequently isolated from clinical sources and belong to lineage I (Maury et al., 2019). Group B clonal complexes were chosen because they have been identified epidemiologically as being infrequently isolated from clinical sources and belong to lineage II (Maury et al., 2019). Elucidating the *inlA* and SSI-1 profile of these clonal complexes, and how these clonal complexes associate with adhesion at a food industry-relevant temperature, would allow us to understand the evolutionary relationship of the adhesion phenotype in *L. monocytogenes* and lessen concerns surrounding confounding factors in the genome.

Another tool to find potentially confounding genes is the genome-wide association study (GWAS), which can associate a phenotype to loci in the genome, potentially uncovering genes which were previously unknown to play a role (Lees et al., 2018). A GWAS of *L. monocytogenes* adhesion could provide insight into the genes *L. monocytogenes* uses to adhere to surfaces.

An investigation into the associations of adhesion at 8 °C with the pangenome, clonal complexes, and genes of interest will yield valuable information about phenotype prediction, potential adhesion mechanisms, and the evolution of the adhesion phenotype in *L. monocytogenes*. Accordingly, the objectives of this study are to (i) identify potential associations between adhesion phenotype at 8 °C and *inlA* genotype, SSI-1 presence, and clonal complexes; (ii) perform a GWAS to identify pangenome elements associated with adhesion phenotype; and (iii) identify potential associations between planktonic growth at 8 °C and *inlA* genotype, SSI-1 presence, and clonal complex.

2. Materials and methods

2.1. Bacterial isolates and growth conditions

Two groups of *Listeria monocytogenes* isolates were used in this study (n = 184). Among these, Group 1 (isolates from animal, environmental, food, and human sources in Canada and Switzerland, n = 122) had been previously sequenced and phenotypically characterized (P. Hingston et al., 2017). Isolates from group 2 (n = 62) came from irrigation water in the lower mainland of British Columbia, Canada (Falardeau et al., 2017). Isolates were stored at −80 °C in brain heart infusion broth (Difco™, Fisher Scientific, Canada) and 25% glycerol (Fisher Scientific, Canada) and were routinely cultured on brain heart infusion agar (BHIA, Difco™, Fisher Scientific, Canada).

2.2. Cold growth and adhesion assay

Listeria monocytogenes cultures were grown for 18–20 h at 22 °C in three biological replicates. The cultures were then standardized to 10^9 CFU/mL through spectrophotometric evaluation and diluted to 10^5 CFU/mL in brain heart infusion broth. The cultures were then inoculated into tissue culture treated polystyrene 96 well plates (Falcon® Multiwell Flat-Bottom Plates with Lids, Sterile, Corning®) in four technical replicates. The plates were incubated at 8 °C and 100% relative humidity for 15 days, and the optical density (OD) at 600 nm was measured every 24 h using a plate reader (Spectramax, V6.3; Molecular Devices, Sunnyvale, CA). Upon completion of the growth period, the media and suspended cells were removed from the plate, and the wells were washed three times with excess 0.05M TRIS buffer adjusted to pH 7.4. Adherent cells were stained with 0.1% crystal violet solution for 30 min. The wells were washed again three times with excess 0.05M TRIS buffer adjusted to pH 7.4. Adherent crystal violet was eluted with 95% ethanol for 30 min and quantified spectrophotometrically at 595 nm using a plate reader (Spectramax, V6.3; Molecular Devices, Sunnyvale, CA).

2.3. Whole genome sequencing

Group 1 was previously sequenced on an Illumina Hi-Seq platform (P. Hingston et al., 2017). For group 2 isolates, genomic DNA was extracted using the PureLink™ Genomic DNA Mini Kit (Thermo Fisher Scientific) and sequenced using the Illumina Hi-Seq Platform at Genome Quebec. Raw reads were trimmed using Trimmomatic version 0.39 (using default parameters for paired-end reads) and uploaded to the NCBI Sequence Read Archive (SRA) under Bioproject PRJNA616119 (Bolger et al., 2014; Leinonen et al., 2010). FastQC version 0.11.4 (https://www.bioinformatics.babraham.ac.uk/projects/fastqc/) was used to ensure that the quality of the resulting trimmed reads was adequate. Trimmed reads were assembled using SPAdes version 3.13.0, using *k*-mer sizes of 21, 33, 55, 77, 99, and 127, and the “careful” option (Bankevich et al., 2012).

2.4. Genotyping of inlA and SSI-1 identification

Premature stop codons (PMSCs) and deletions in *inlA* were identified using NCBI's blastx command in BLAST version 2.2.31+ (Camacho et al., 2009). First, a full length *inlA* amino acid sequence from *L.* monocytogenes EGD-e was downloaded from NCBI and used as a reference sequence (NCBI accession number GCA_000196035.1). Then, using blastx, this *inlA* sequence was queried against the assembled genomes used in this study. NCBI's blastx returned an asterisk in the location of any premature stop codons and a dash for a deletion of a codon (Camacho et al., 2009). Using custom scripts, the locations of these PMSCs and deletions were identified. The presence or absence of SSI-1 was assessed using NCBI's blastn. First, the SSI-1 nucleotide sequence from *L.* monocytogenes EGD-e was downloaded from NCBI as a reference sequence (NCBI accession number GCA_000196035.1). Then, using blastn, this SSI-1 sequence was queried against the assembled genomes used in this study, and using custom scripts, the presence or absence of an alignment result was obtained for all genomes queried (Camacho et al., 2009). SSI-1 was deemed present if the reference sequence aligned to an 8766bp fragment with ≥99.5% identity and ≥95% coverage and was deemed absent if there was no alignment (<1e-05 e-value threshold). This successfully identified the presence or absence of SSI-1 in 158 of 184 isolates. The genome assemblies of the remaining 26 isolates did not assemble into long, high-quality contigs at this locus and resulted in short alignments to the SSI-1 sequence (≥1e-05 e-value); therefore, the presence or absence of SSI-1 in these isolates was confirmed by PCR.

2.5. SSI-1 presence determination by PCR

All PCRs were done using Q5® High-Fidelity DNA Polymerase (New England Biolabs, MA, USA) and their recommended reaction and thermocycling conditions for routine PCR. First, the 26 isolates were screened for one of the genes in SSI-1, *gadD1*, using primers that had been previously designed (Hein et al., 2011). Of these, four genomes contained *gadD1* and were confirmed to have the remaining four genes in SSI-1 using primers designed using NCBI's Primer-BLAST tool (Ye et al., 2012). Primers used can be found in Table 2.

2.6. Maximum likelihood phylogeny and multi locus sequence typing

A reference free, maximum likelihood phylogeny was constructed using the kSNP3.0 maximum likelihood phylogeny output with a *k-mer* size of 19 selected as the optimal *k-mer* size using K chooser (Gardner et al., 2015). The resulting ML phylogeny was rooted using LSD2 v. 1.4.2.2, using (i) tip dates that corresponded to the year of isolation for each strain; (ii) a substitution rate of 2.5E-7 substitutions/site/year; (iii) constrained mode, with the root estimated using constraints on all branches (-r as); (iv) variances applied to all branch lengths (-v 2); (v) 10,000 samples for calculating confidence intervals for estimated dates (-f 10000) (Moura et al., 2016; To et al., 2016). A heat map was added to this phylogeny to indicate *inlA* genotype, SSI-1 presence, and group A or group B clonal complex using the bactaxR package in R (Laura M Carroll et al., 2020). Seven gene multi-locus sequence typing was done using seq2mlst (https://github.com/lmc297/seq2mlst), and clonal complexes were determined using the PasteurMLST database scheme (Laura M. Carroll, 2017; Jolley and Maiden, 2010).

Table 2
Oligonucleotides used to identify SSI-1 presence.

Primer	Sequence 5′ to 3′	Target	Source
gadD1 F	GGT ATT GTG GGT ATT CTG G	gadD1	Hein et al. (2011)
gadD1 R	CTG ACC GAT AAT CTG ACT C	gadD1	Hein et al. (2011)
lmo0444 F	AAA TTG CGG ATG GCG GAA AC	lmo0444	this study
lmo0444 R	TCG CGC TAC CTA CTG CTT TT	lmo0444	this study
lmo0445 F	GAG ACG ACG ATT CGG AGG TC	lmo0445	this study
lmo0445 R	AAA TCA CAT CTG CTT GCG GC	lmo0445	this study
lmo0446 F	GTT GGA GCG GGA AGA GAG TT	lmo0446	this study
lmo0446 R	TTC GAT GCG TGG CGT ATT TG	lmo0446	this study
lmo0448 F	CGG CTG GGT TAG TAA GAC GC	lmo0448	this study
lmo0448 R	ATA CGT TGT TAC CAC CGC CG	lmo0448	this study

2.7. Genome-wide association study

Pyseer version 1.3.4 was used to perform a genome wide association study with the 8 °C adhesion phenotype data (Lees et al., 2018). First, a file containing *k*-mers from the *L. monocytogenes* pangenome for the 184 isolates included here was created using fsm-lite version 1.0, which used the assembled genomes of the isolates as input. *K*-mers are short sequences of length *k* which can be compared to phenotype data in a GWAS as well as many other bioinformatic analyses. A distance matrix was created using Mash version 2.2.2 in order to correct for population structure variance to avoid spurious results coming from the natural sequence variability in our collection of *L. monocytogenes* (Lees et al., 2016; Ondov et al., 2016). The distance matrix, pangenome *k*-mers, and continuous phenotype data were inputted into Pyseer to perform a fixed effect association model, and the significance threshold was adjusted for multiple comparisons using a Bonferroni correction (Lees et al., 2018). The resulting significant *k*-mers were aligned to their respective genes using NCBI blast.

2.8. Statistical analyses

Cold growth and adhesion assay data were analysed and visualized using R version 3.5.2 with the Growthcurver and tidyverse packages (Sprouffske and Wagner, 2016). Phenotype data (adhesion or growth parameters) was compared among *inlA* and clonal complex genotypes

Table 1
Kmers that associate significantly with *L. monocytogenes* adhesion at 8 °C. The genome wide association study was done using Pyseer version 1.3.4 and alignments with NCBI blast.

Kmer	Aligned gene product(s)	NCBI accession number	Gene function	Source
TTTTTTCCTTCTT	Glycoside hydrolase family 31 protein	CP014252.2	Exact function unknown	Consortium (2019)
TTCATATGAAG	Ribosome maturation factor RimP	CP014252.2	Protein synthesis	Nelson et al. (2004)
TTACCTCTGTT	ATP-binding cassette domain-containing protein	CP014252.2	Exact function unknown	Consortium (2019)
	AAA family ATPase		Exact function unknown	Consortium (2019)
TGCGTATGTG	Cardiolipin synthase	CP006596.2	Increasing membrane fluidity	(P. A. Hingston et al., 2015)
GTCGATCCGGCCG	S1 RNA-binding domain- containing protein	CP014252.2	Exact function unknown	Consortium (2019)
CGCGCTGCACGCGG	3D-(3,5/4)-trihydroxycyclohexane- 1,2-dione acylhydrolase (decyclizing)	CP032669.1	Myo-inositol metabolism	Consortium (2019)
CATTCCCGCTGT	Superoxide dismutase	CP048400.1	Oxidative stress response	(P. A. Hingston et al., 2015; Suo et al., 2012)
ACATTAAACGTT	Helicase	CP014250.2	DNA replication	Consortium (2019)
	Leucine-tRNA ligase		Protein synthesis	Consortium (2019)

using a one-way ANOVA followed by Tukey's honest significant difference test. As there are only two categorical variables for the SSI-1 genotype, Welch's *t*-test was used. GWAS statistical analyses were performed using Pyseer and include multiple linear regressions with a fixed effects model and a Bonferroni correction for multiple comparisons (Lees et al., 2018).

2.9. Data availability

Whole genome sequencing data can be found under NCBI BioProject accession number PRJNA616119. Experimental data can be found in Table S1.

3. Results

3.1. *inlA* and SSI-1 genotypes are not uniformly distributed among clonal complexes

A collection of *L. monocytogenes* isolates (n = 184) from animal, environmental, water, food, and human sources was used. A maximum likelihood phylogeny of the *L. monocytogenes* isolates showed that the majority of isolates belonged to lineage I and lineage II, with one isolate belonging to lineage III (Fig. 1). Genotyping of *inlA* in all isolates revealed that 79.3% (n = 146) had a full length *inlA*, 9.8% (n = 18) had a truncated *inlA*, 8.7% (n = 16) had a 3CD *inlA*, and 2.2% (n = 4) had a 9aa PMSC *inlA* (Fig. 1). Interestingly, when genotyping the *inlA* and internalin B (*inlB*) operon, in two of the isolates (1.1%), a deletion of 47

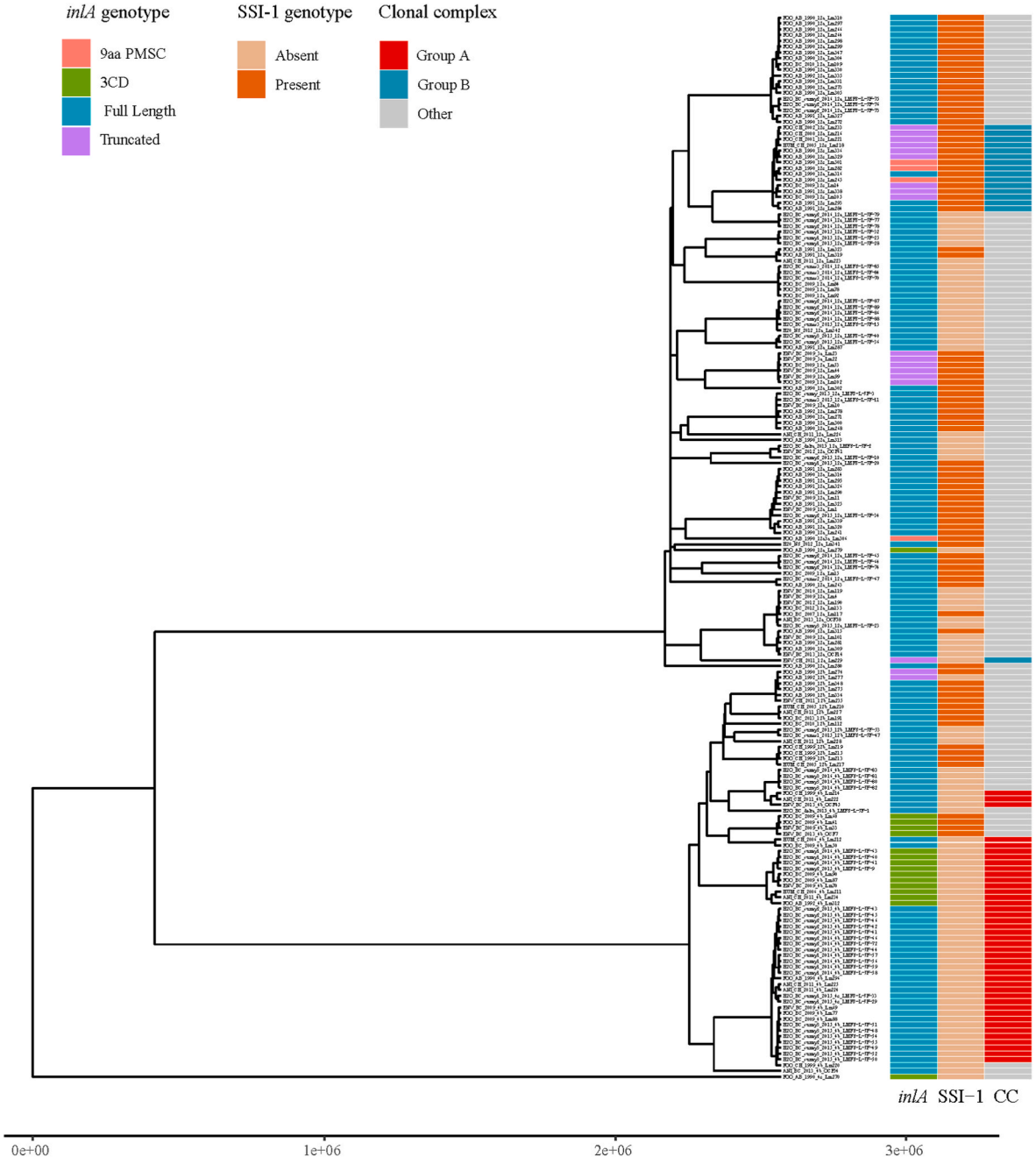

Fig. 1. Reference free kmer based maximum likelihood phylogenetic tree created using kSNP version 3.0 and rooted using LSD2 v. 1.4.2.2 n = 184, branch lengths are reported in years. The genotype heatmap describes each strain's *inlA* genotype, SSI-1 genotype, and clonal complex and was created using bactaxR.

amino acids was found in *inlB* at position 355, removing a large portion of the B repeats region. Within the genomes available on NCBI, 1.3% (n = 38 of 2974) also contained this deletion at position 355. Although uncommon, a deletion of this size would likely alter the function of this important virulence gene and therefore, the *inlB* locus was included for further analyses in this study. Among all isolates, 49.5% (n = 91) contained SSI-1 (Fig. 1). In the collection of *L. monocytogenes* isolates, 42 isolates belonged to group A clonal complexes and 16 isolates belonged to group B clonal complexes (Fig. 1). Of the isolates within group A clonal complexes, 76.2% had a full length *inlA*, while the remaining 23.8% (n = 10 of 42) had a 3CD *inlA* (Fig. 1). No isolates within group A clonal complexes had SSI-1 (Fig. 1). In contrast, of the isolates within group B clonal complexes, only 18.8% (n = 3 of 16) had a full length *inlA*, while 62.5% (n = 10 of 16) had a truncated *inlA* and 18.8% (n = 3 of 16) had a 9aa PMSC *inlA* (Fig. 1). Among group B isolates, 93.8% (n = 15 of 16) had SSI-1. In summary, isolates assigned to group A clonal complexes were more likely to have a 3CD *inlA* genotype (23.8%), as compared to the entire *L. monocytogenes* collection (8.7%), while isolates assigned to group B clonal complexes were more likely to have a truncated *inlA* genotype (62.5%), as compared to the entire *L. monocytogenes* collection (9.8%).

3.2. Adherence at 8 °C differed based on inlA genotype, SSI-1 presence, and clonal complex

Isolates with truncated *inlA* had the highest mean adhesion (0.52 ± 0.15 ABS_{595nm}). These isolates adhered significantly more (Tukey HSD, $P < 0.0001$) than isolates with full length *inlA* (0.36 ± 0.18) or 3CD *inlA* (0.16 ± 0.09) (Fig. 2 A). Additionally, isolates with 9aa PMSC *inlA* (0.42 ± 0.17) were not significantly different from isolates with truncated *inlA* (Fig. 2 A). Isolates with the 47 amino acid deletion in *inlB* identified in this study did not adhere differently (0.46 ± 0.09; Welch's *t*-test, $P > 0.05$) than isolates with a full length *inlB* (0.36 ± 0.19) (Fig. 2 D). Isolates with SSI-1 (0.43 ± 0.18) adhered significantly (Welch's *t*-test, $P < 0.0001$) more than isolates without SSI-1 (0.30 ± 0.17) (Fig. 2 B). Moreover, group B clonal complexes adhered significantly (Tukey HSD, $P < 0.0001$) more than group A clonal complexes (Fig. 2 C).

3.3. Association of the pangenome and adhesion at 8 °C

A genome-wide association study (GWAS) was conducted to associate adhesion at 8 °C with loci in the *L. monocytogenes* genome. Eight *k*-mers were identified to be significantly associated with adhesion at 8 °C (Table 1). Five of these *k*-mers aligned to gene products with known functions. Additionally, the function of these genes could support adhesion at low temperatures. These functions included protein synthesis, membrane fluidity alterations, myo-inositol metabolism, DNA replication, and oxidative stress response (Table 1). Three significantly associated *k*-mers aligned to genes of uncharacterized function; these included a glycoside hydrolase family 31 protein, an ATP-binding cassette domain-containing protein, a AAA family ATPase, and a S1 RNA-binding domain-containing protein (Table 1).

3.4. Growth rate was associated with group B clonal complexes and inlA genotype, but not SSI-1

Three growth parameters were evaluated: growth rate, carrying capacity (maximum growth density, N_{max}), and time to the midpoint of the exponential phase (reflective of lag phase and growth rate, T_{mid}). It was observed that the growth rate of truncated *inlA* isolates (0.079 ± 0.025 h^{-1}) was significantly higher (2-fold) than isolates with 3CD *inlA* and full length *inlA* (Tukey HSD, $P < 0.0001$) (Fig. 3 A). 3CD *inlA* isolates were observed to have the lowest growth rate (0.039 ± 0.015 h^{-1}), being significantly different from truncated *inlA* only (Tukey HSD, $P < 0.0001$) (Fig. 3 A). The growth rate of 9aa PMSC *inlA* isolates was not significantly different from any other *inlA* genotype (Fig. 3 A). No significant differences in N_{max} or T_{mid} were observed when isolates were grouped by *inlA* genotype (Fig. 4 A, Fig. 5 A). It was observed that isolates with SSI-1 did not have a significantly different growth rate than isolates without SSI-1 (Fig. 3 B). Presence of SSI-1 was associated with significantly lower N_{max} (Welch's *t*-test, $P < 0.005$) and significantly lower T_{mid} (Welch's *t*-test, $P < 0.0005$); however, the magnitude of these differences was very low (Figs. 4 B, Fig. 5 B). When grouping isolates by clonal complex, significant differences were observed (Welch's *t*-test, $P < 0.0001$) in growth rate between Group B and Group A clonal complexes (Fig. 3 C). No significant differences were observed amongst the group B and group A clonal complexes in N_{max} (Fig. 4 C). Group A clonal complexes had a significantly higher T_{mid} (Welch's *t*-test, $P < 0.05$); however, the magnitude of these differences was low (Fig. 5 C).

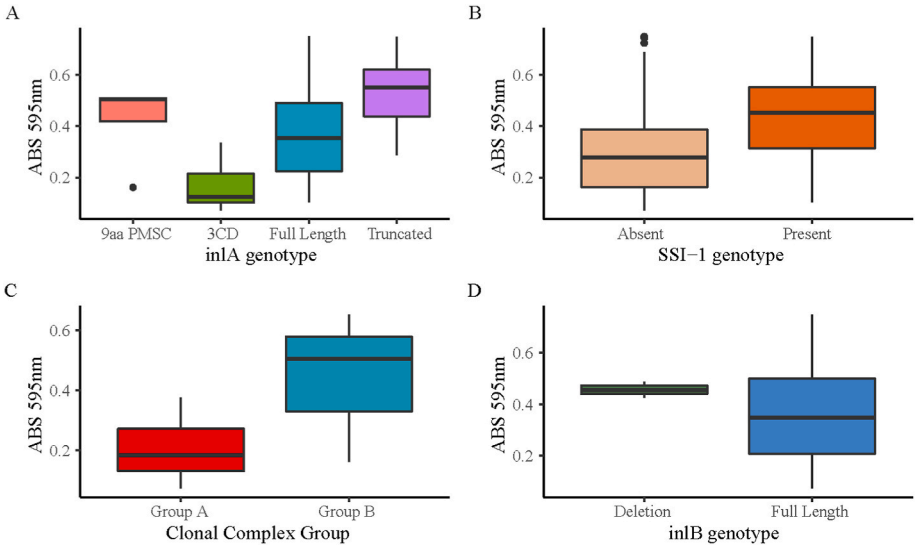

Fig. 2. Quantity of adhered *L. monocytogenes* at 8 °C on polystyrene in brain heart infusion broth grouped by (A) inlA genotype, (B) SSI-1 presence, (C) clonal complex and (D) inlB genotype. Summary statistics shown are the median, interquartile range (IQR), the whiskers represent 1.5 • 25th and 75th percentiles, and data falling outside the whiskers are plotted individually.

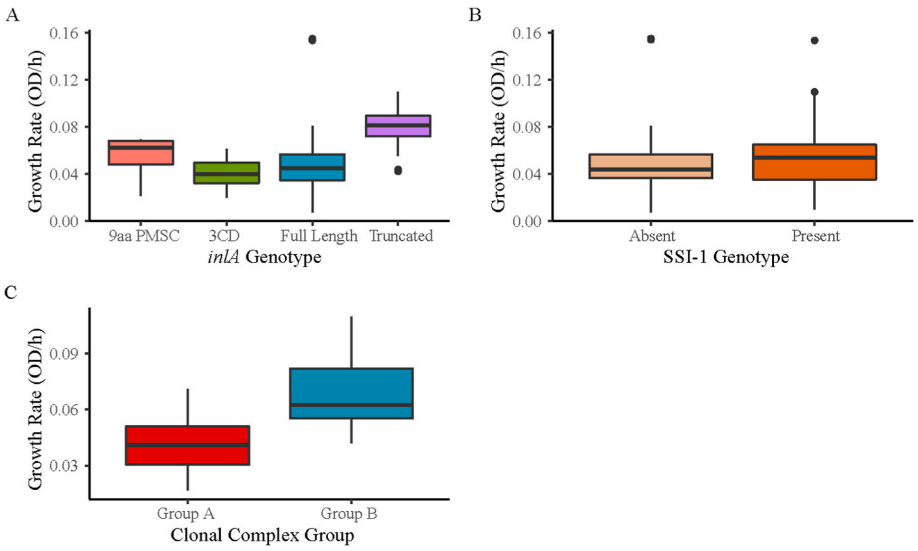

Fig. 3. Growth rate of *L. monocytogenes* at 8 °C in brain heart infusion broth grouped by (A) inlA genotype, (B) SSI-1 presence, and (C) clonal complex. OD was measured at 600 nm. Summary statistics shown are the median, interquartile range (IQR), the whiskers represent 1.5 • 25th and 75th percentiles, and data falling outside the whiskers are plotted individually.

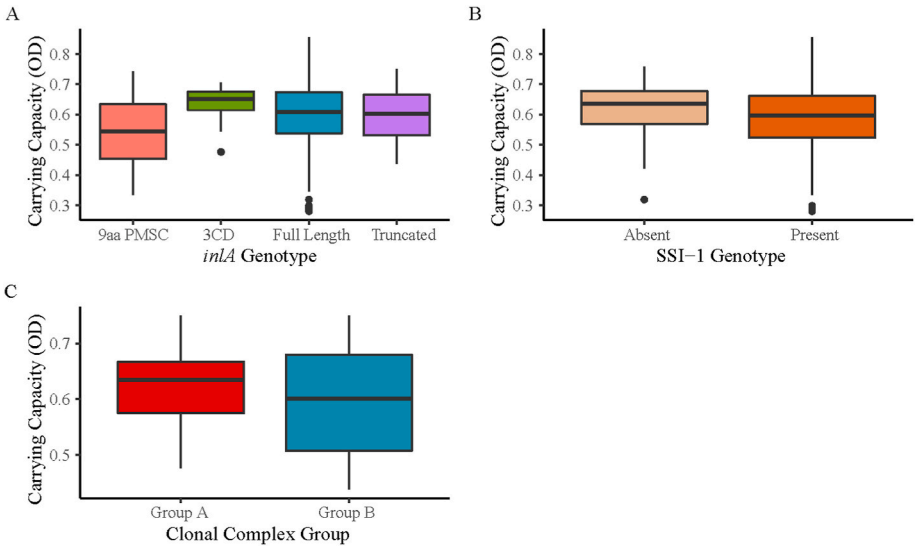

Fig. 4. Carrying capacity of *L. monocytogenes* at 8 °C in brain heart infusion broth grouped by (A) inlA genotype, (B) SSI-1 presence, and (C) clonal complex. OD was measured at 600 nm. Summary statistics shown are the median, interquartile range (IQR), the whiskers represent 1.5 • 25th and 75th percentiles, and data falling outside the whiskers are plotted individually.

4. Discussion

4.1. Disease-associated clonal complexes are associated with invasion-enhancing inlA mutations and SSI-1 absence

Group A clonal complexes (CC1, CC2, CC4, and CC6) have been shown to be the most frequent clonal complexes in clinical isolations of *L. monocytogenes* and have been called hypervirulent (Maury et al., 2019). Group B clonal complexes (CC9 and CC121) have been shown to be infrequent clonal complexes in clinical isolations of *L. monocytogenes* and have been called hypovirulent (Maury et al., 2019). Genotyping found that group A was more than twice as likely, compared to the entire *L. monocytogenes* collection, to have a 3CD *inlA* and did not have truncated *inlA*. Meanwhile, group B was over six times as likely, compared to the entire *L. monocytogenes* collection, to have a truncated *inlA* and did not have 3CD *inlA* (Fig. 1). Phylogenetically, groups A and B are clustered into distinct groups in lineage I and II respectively (Fig. 1). These results show that hypervirulent group A clonal complexes are associated with 3CD *inlA*, and such strains have demonstrated increased invasion of intestinal epithelium cells (Kovacevic et al., 2013). This could be a mechanism to explain why group A clonal complexes are more frequently seen in clinical sources. Our results also confirm that hypovirulent group B clonal complexes are associated with truncated *inlA*, which is a known cause of attenuated virulence in *L. monocytogenes* (Jacquet et al., 2004). Interestingly, the B-repeats deletion in *inlB* identified in this study was found in two strains with truncated *inlA*. Additionally, 35 of the 38 strains with the B-repeats deletion in *inlB* identified in the genomes available on NCBI (n = 2974) had a truncated *inlA*. This suggests that, in addition to the evolutionary pressure on *inlA* towards attenuated virulence function, perhaps *inlB* and other virulence genes also have an evolutionary pressure towards attenuated virulence in strains with truncated *inlA*. InlB is responsible for internalization into

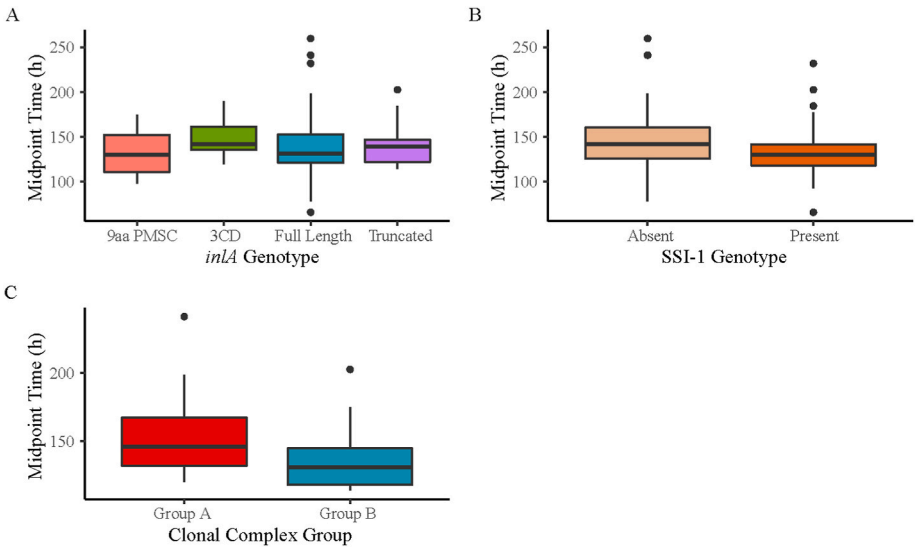

Fig. 5. Midpoint time of *L. monocytogenes* at 8 °C in brain heart infusion broth grouped by (A) inlA genotype, (B) SSI-1 presence, and (C) clonal complex. Summary statistics shown are the median, interquartile range (IQR), the whiskers represent 1.5 • 25th and 75th percentiles, and data falling outside the whiskers are plotted individually.

endothelial membranes (Parida et al., 1998). If *inlA* is not functional, *L. monocytogenes* will not be able to cross epithelial membranes in order to gain entry into the body (Nightingale et al., 2008). In strains where *inlA* is non-functional, *L. monocytogenes* would rarely encounter an endothelial membrane; thus, evolutionary pressure for maintenance of a functional *inlB* could potentially be relieved, and *inlB* would become a vestigial gene. An investigation into the virulence function of the B-repeats deletion *inlB* and an investigation into other virulence genes would yield valuable insights into the evolutionary pressures on *L. monocytogenes*. SSI-1 was found to be less prevalent in strains with group A clonal complexes; additionally, strains with group A clonal complexes have been shown to be adapted to parasitism of animals and humans (Maury et al., 2019). It is therefore plausible that possession of SSI-1 would not be an evolutionary advantage. Conversely, group B clonal complexes were more likely to have SSI-1 and have been shown to be adapted to high stress environments, such as acidic and salty food products, where there is a clear advantage in SSI-1 conferring increased resistance to stressors (Keeney et al., 2018; Maury et al., 2019; Ryan et al., 2010).

4.2. Hypothetical adhesion mechanisms of inlA and SSI-1

It was observed that at 8 °C, strains with truncated *inlA*, and to a certain extent, those with 9aa PMSC *inlA*, showed increased adherence compared to other *inlA* genotypes. (Fig. 2 A). This association of truncated *inlA* and adhesion does not concur with research conducted at 37 °C suggesting truncated *inlA* strains do not have an increased adhesion phenotype compared to full length *inlA* (Keeney et al., 2018; Wang et al., 2015). However, this association does concur with research conducted at 37 °C suggesting truncated *inlA* proteolysis products play a direct role in the increased adhesion phenotype (Franciosa et al., 2009). If *inlA* proteolysis products are leading to an increase in biomass in the extracellular space, full length *inlA* and 3CD *inlA* remaining membrane bound could result in less proteolysis of *inlA* in these strains. The results suggest that at low temperatures, strains with truncated *inlA* may pose the greatest risk of persistence in a food production facility. The association of *inlA* genotype and adhesion, in addition to the established causal associations with *inlA* genotype and virulence, make *inlA* a unique marker gene with which one could identify *L. monocytogenes* in a sample, and make predictions regarding virulence and adhesion capacity (Nightingale et al., 2008). Additionally, these associations indicate that mutations leading to attenuated virulence (truncated *inlA*) are associated with increased adhesion, while mutations leading to increased virulence (3CD *inlA*) are associated with decreased adhesion (Kovacevic et al., 2013; Nightingale et al., 2008). It was observed that strains with SSI-1 adhered more at 8 °C than strains without SSI-1 (Fig. 2 B). At 30 °C, it was also observed that strains with SSI-1 adhered more than strains without SSI-1 (Keeney et al., 2018). This suggests there is a possibility a gene in SSI-1 may provide an adhesion mechanism. SSI-1 consists of five genes, lmo0444-lmo0448 (Ryan et al., 2010). Previously described functions among SSI-1 genes include lmo0445 being shown to regulate the transcription of the SSI-1 operon, lmo0446 encoding a bile tolerance protein, and lmo0447-8 forming a part of the glutamate decarboxylase acid resistance system (Begley et al., 2005; Cotter et al., 2005). The remaining gene in SSI-1, lmo0444, has been characterized *in silico* and has homologous regions to transmembrane domains, a reovirus attachment protein, and a phage infection protein (Consortium, 2019). Lmo0444 is the most promising hypothetical causal gene within SSI-1 which could explain the observed association with increased adhesion and thereby merits further investigation (Fig. 2 B).

4.3. Disease-associated clonal complexes are associated with decreased adhesion ability

Group B clonal complexes were observed to adhere substantially more than Group A clonal complexes (Fig. 2 C). This suggests that hypervirulent clonal complexes adhere less. Conversely, hypovirulent clonal complexes are associated with increased adhesion ability. This also shows that the adhesion phenotype clusters in phylogenetically distinct groups which have genetic traits in common, such as clonal complex, *inlA* genotype, and SSI-1 presence (Figs. 1 and 2 A, B, C). The strong association of adhesion and clonal complex suggests that MLST is an effective tool to predict adhesion phenotype and has the potential to be used routinely as sequencing becomes more prevalent.

4.4. Genome-wide association revealed potential genes responsible for L. monocytogenes adhesion at 8 °C

Some gene functions associated with adhesion at 8 °C are consistent with previous literature including protein synthesis (Consortium, 2019; Nelson et al., 2004), increasing membrane fluidity (P. A. Hingston, Piercey and Hansen, 2015), myo-inositol metabolism (Consortium,

2019), DNA replication (Consortium, 2019), and oxidative stress response (Consortium, 2019) (Table 1). DNA replication and protein synthesis genes are responsible for growth and proliferation, while myo-inositol metabolism genes are reflective of the metabolism of metabolites in brain heart infusion broth (Consortium, 2019). Growth and metabolic activity would naturally be associated with increased cell density adhered to a surface, increased membrane fluidity would enhance the ability of a microorganism to proliferate when temperature is reduced, and many studies have shown that the ability to reduce oxidative stress is needed in *L. monocytogenes* to effectively adhere to surfaces (P. A. Hingston et al., 2015; Suo et al., 2012). The remaining gene functions significantly associated to adhesion at 8 °C have not been reported and have only been characterized by amino acid homology. These include a glycoside hydrolase family 31 protein (Consortium, 2019), an ATP-binding cassette domain-containing protein (Consortium, 2019), an AAA family ATPase (Consortium, 2019), and a S1 RNA-binding domain-containing protein (Table 1) (Consortium, 2019). Further functional characterizations (e.g. via knockout mutants) could further reveal the role of these genes in *L. monocytogenes* adhesion at 8 °C.

4.5. Group B clonal complexes and truncated inlA strains grow faster at 8 °C

We observed that strains belonging to Group B clonal complexes had higher growth rates than strains belonging to group A clonal complexes (Fig. 3 C). Additionally, the growth rate of truncated *inlA* isolates was two-fold higher than full-length and 3CD *inlA* isolates. (Fig. 3 A). This suggests that strains with these genotypes may be able to grow faster in food products or establish themselves more quickly in a food processing plant niche. Using strain *inlA* genotype and clonal complex as a marker for cold growth rate would be relevant to food industries where refrigeration is one of the main controls against pathogen growth in ready to eat foods, such as fresh produce. Due to the lack of evidence suggesting *inlA* or SSI-1 play a causal role in cold growth in *L. monocytogenes*, the associations observed with growth rate at 8 °C are likely due to other confounding genomic factors. Importantly, what this association does indicate is that strains with genotypes associated with decreased virulence grow faster at 8 °C than strains with genotypes associated with increased virulence. Additionally, the lack of associations between the genotypes examined and N_{max} indicate that all isolates grew to similar cell densities; therefore, cell density differences do not account for the observed differences in adhesion.

4.6. There may be an evolutionary trade off between virulence and adhesion at 8 °C in L. monocytogenes

When an organism gains fitness in a phenotype at the expense of another phenotype, this is an evolutionary trade off (Allaby, 2010). Examples of trade offs have been found in many organisms including *L. monocytogenes*. For example, it was found that upon challenge with a bacteriophage, *L. monocytogenes* mutated and changed its teichoic acid glycosylation (Sumrall et al., 2019). This prevented the bacteriophage from parasitizing the bacterium; however, the mutation also prevented *inlB* from associating with the cell wall, impairing invasion into human endothelial cells, and consequently reducing virulence fitness (Sumrall et al., 2019). The study found that resistance to a bacteriophage stressor came at the cost of virulence (Sumrall et al., 2019). Similarly, the 8 °C adhesion phenotype and genotype analyses above provide evidence there may be an evolutionary trade off in *L. monocytogenes* between virulence and adhesion at cold temperatures. We see that clonal complexes with high clinical frequency (group A) are more likely to have a 3CD *inlA*, which enhances virulence, and are less likely to have SSI-1, which aids in stress survival (Fig. 1). Conversely, clonal complexes with low clinical frequency (group B) are more likely to have a truncated *inlA*, which impairs virulence, and are more likely to have SSI-1, which aids in stress survival (Fig. 1). We see that clonal complexes with high clinical frequency (group A) associate negatively with adhesion at 8 °C, and clonal complexes with low clinical frequency (group B) associate positively with adhesion at 8 °C (Fig. 2 C). We see that strains with truncated *inlA* adhere the most and grow the fastest at 8 °C, and that in some of these strains, there is a 47 amino acid deletion in *inlB*, which may impair the virulence function of this gene as well (Figs. 3 A, Fig. 2 D). Finally, we see that strains with 3CD *inlA* adhered the least and grow the slowest at 8 °C (Figs. 3 A, Fig. 2 A). Full length *inlA* is the ancestor of all *inlA* genotypes discussed (Ragon et al., 2008). This supports that within *L. monocytogenes* lineage I, there are subtypes pressured to have an *inlA* genotype that increases virulence, which is coming at the cost of adhesion (Fig. 2 A). Conversely, within *L. monocytogenes* lineage II, there are subtypes pressured to have a less virulent *inlA* at the gain of adhesion (Fig. 2 A). Strains with full length *inlA* may be in an intermediate state within the continuing divergent evolution of lineages I and II.

5. Conclusions

In this study, we have shown that strains with truncated *inlA*, SSI-1, and clonal complexes with low clinical frequency are associated with increased growth rates and increased adhesion at 8 °C. Furthermore, strains with 3CD *inlA*, no SSI-1, and clonal complexes with high clinical frequency are associated with decreased growth rate and decreased adhesion at 8 °C. These results support that there is an evolutionary trade off between virulence and adhesion at 8 °C in *L. monocytogenes*. Future research into the virulence and evolution of the 47 amino acid deletion of the B repeats region in *inlB*, the adhesion mechanism of SSI-1 and *inlA*, and the functions of genes identified through genome-wide association, will allow us to further understand *L. monocytogenes* evolution and biology, which will inform policy-making on mitigating the food safety risks of *L. monocytogenes*.

Declaration of competing interest

The authors declare that they have no known competing financial interests or personal relationships that could have appeared to influence the work reported in this paper.

Acknowledgements

This research was supported by the Natural Sciences and Engineering Research Council of Canada (NSERC Discovery Grant RGPIN-2015-04871). We thank Dr. Vic Gannon at the Public Health Agency of Canada and Dr. Taurai Tasara at University of Zurich for providing some of the *Listeria monocytogenes* isolates used in this study.

Appendix A. Supplementary data

Supplementary data to this article can be found online at https://doi.org/10.1016/j.fm.2021.103915.

References

Allaby, M., 2010. A Dictionary of Ecology. Oxford University Press.
Bankevich, A., Nurk, S., Antipov, D., Gurevich, A.A., Dvorkin, M., Kulikov, A.S., Prjibelski, A.D., 2012. SPAdes: a new genome assembly algorithm and its applications to single-cell sequencing. J. Comput. Biol. 19 (5), 455–477.
Begley, M., Sleator, R.D., Gahan, C.G., Hill, C., 2005. Contribution of three bile-associated loci, bsh, pva, and btlB, to gastrointestinal persistence and bile tolerance of Listeria monocytogenes. Infect. Immun. 73 (2), 894–904.
Bolger, A.M., Lohse, M., Usadel, B., 2014. Trimmomatic: a flexible trimmer for Illumina sequence data. Bioinformatics 30 (15), 2114–2120.
Camacho, C., Coulouris, G., Avagyan, V., Ma, N., Papadopoulos, J., Bealer, K., Madden, T.L., 2009. BLAST+: architecture and applications. BMC Bioinf. 10 (1), 421.
Carroll, L.M., 2017. seq2mlst: in Silico Multi-Locus Sequence Typing, Version 1.0.1.

Carroll, L.M., Wiedmann, M., Kovac, J., 2020. Proposal of a taxonomic nomenclature for the Bacillus cereus group which reconciles genomic definitions of bacterial species with clinical and industrial phenotypes. mBio 11 (1).
Consortium, U., 2019. UniProt: a worldwide hub of protein knowledge. Nucleic Acids Res. 47 (D1), D506–D515.
Cotter, P.D., Ryan, S., Gahan, C.G., Hill, C., 2005. Presence of GadD1 glutamate decarboxylase in selected Listeria monocytogenes strains is associated with an ability to grow at low pH. Appl. Environ. Microbiol. 71 (6), 2832–2839.
Falardeau, J., Johnson, R.P., Pagotto, F., Wang, S., 2017. Occurrence, characterization, and potential predictors of verotoxigenic Escherichia coli, Listeria monocytogenes, and Salmonella in surface water used for produce irrigation in the Lower Mainland of British Columbia, Canada. PloS One 12 (9).
Franciosa, G., Maugliani, A., Scalfaro, C., Floridi, F., Aureli, P., 2009. Expression of internalin A and biofilm formation among Listeria monocytogenes clinical isolates. Int. J. Immunopathol. Pharmacol. 22 (1), 183–193.
Gardner, S.N., Slezak, T., Hall, B.G., 2015. kSNP3. 0: SNP detection and phylogenetic analysis of genomes without genome alignment or reference genome. Bioinformatics 31 (17), 2877–2878.
Harrand, A.S., Jagadeesan, B., Baert, L., Wiedmann, M., Orsi, R.H., 2020. Evolution of Listeria monocytogenes in a food-processing plant involves limited single nucleotide substitutions, but considerable diversification by gain and loss of prophages. Appl. Environ. Microbiol.
Hein, I., Klinger, S., Dooms, M., Flekna, G., Stessl, B., Leclercq, A., Wagner, M., 2011. Stress survival islet 1 (SSI-1) survey in Listeria monocytogenes reveals an insert common to Listeria innocua in sequence type 121 L. monocytogenes strains. Appl. Environ. Microbiol. 77 (6), 2169–2173.
Hingston, P., Chen, J., Dhillon, B.K., Laing, C., Bertelli, C., Gannon, V., Truelstrup Hansen, L., 2017. Genotypes associated with Listeria monocytogenes isolates displaying impaired or enhanced tolerances to cold, salt, acid, or desiccation stress. Front. Microbiol. 8, 369.
Hingston, P.A., Piercey, M.J., Hansen, L.T., 2015. Genes associated with desiccation and osmotic stress in Listeria monocytogenes as revealed by insertional mutagenesis. Appl. Environ. Microbiol. 81 (16), 5350–5362.
Jacquet, C., Doumith, M., Gordon, J.I., Martin, P.M., Cossart, P., Lecuit, M., 2004. A molecular marker for evaluating the pathogenic potential of foodborne Listeria monocytogenes. J. Infect. Dis. 189 (11), 2094–2100.
Jolley, K.A., Maiden, M.C., 2010. BIGSdb: scalable analysis of bacterial genome variation at the population level. BMC Bioinf. 11 (1), 1–11.
Keeney, K., Trmcic, A., Zhu, Z., Delaquis, P., Wang, S., 2018. Stress survival islet 1 contributes to serotype-specific differences in biofilm formation in Listeria monocytogenes. Lett. Appl. Microbiol. 67 (6), 530–536.
Kovacevic, J., Arguedas-Villa, C., Wozniak, A., Tasara, T., Allen, K.J., 2013. Examination of food chain-derived Listeria monocytogenes strains of different serotypes reveals considerable diversity in inlA genotypes, mutability, and adaptation to cold temperatures. Appl. Environ. Microbiol. 79 (6), 1915–1922.
Lecuit, M., Ohayon, H., Braun, L., Mengaud, J., Cossart, P., 1997. Internalin of Listeria monocytogenes with an intact leucine-rich repeat region is sufficient to promote internalization. Infect. Immun. 65 (12), 5309–5319.
Lees, J.A., Galardini, M., Bentley, S.D., Weiser, J.N., Corander, J., 2018. pyseer: a comprehensive tool for microbial pangenome-wide association studies. Bioinformatics 34 (24), 4310–4312.
Lees, J.A., Vehkala, M., Välimäki, N., Harris, S.R., Chewapreecha, C., Croucher, N.J., Tong, S.Y., 2016. Sequence element enrichment analysis to determine the genetic basis of bacterial phenotypes. Nat. Commun. 7 (1), 1–8.
Leinonen, R., Sugawara, H., Shumway, M., Collaboration, I.N.S.D., 2010. The sequence read archive. Nucleic Acids Res. 39 (Suppl. l_1), D19–D21.
Maury, M.M., Bracq-Dieye, H., Huang, L., Vales, G., Lavina, M., Thouvenot, P., Lecuit, M., 2019. Hypervirulent Listeria monocytogenes clones' adaption to mammalian gut accounts for their association with dairy products. Nat. Commun. 10 (1), 1–13.
Moura, A., Criscuolo, A., Pouseele, H., Maury, M.M., Leclercq, A., Tarr, C., Enouf, V., 2016. Whole genome-based population biology and epidemiological surveillance of Listeria monocytogenes. Nat. Microbiol. 2 (2), 1–10.
Nelson, K.E., Fouts, D.E., Mongodin, E.F., Ravel, J., DeBoy, R.T., Kolonay, J.F., Paulsen, I. T., 2004. Whole genome comparisons of serotype 4b and 1/2a strains of the food-borne pathogen Listeria monocytogenes reveal new insights into the core genome components of this species. Nucleic Acids Res. 32 (8), 2386–2395.
Nightingale, K., Ivy, R., Ho, A., Fortes, E., Njaa, B.L., Peters, R., Wiedmann, M., 2008. inlA premature stop codons are common among Listeria monocytogenes isolates from foods and yield virulence-attenuated strains that confer protection against fully virulent strains. Appl. Environ. Microbiol. 74 (21), 6570–6583.
Ondov, B.D., Treangen, T.J., Melsted, P., Mallonee, A.B., Bergman, N.H., Koren, S., Phillippy, A.M., 2016. Mash: fast genome and metagenome distance estimation using MinHash. Genome Biol. 17 (1), 132.
Parida, S.K., Domann, E., Rohde, M., Müller, S., Darji, A., Hain, T., Chakraborty, T., 1998. Internalin B is essential for adhesion and mediates the invasion of Listeria monocytogenes into human endothelial cells. Mol. Microbiol. 28 (1), 81–93.
Ragon, M., Wirth, T., Hollandt, F., Lavenir, R., Lecuit, M., Le Monnier, A., Brisse, S., 2008. A new perspective on Listeria monocytogenes evolution. PLoS Pathog. 4 (9).
Ryan, S., Begley, M., Hill, C., Gahan, C., 2010. A five-gene stress survival islet (SSI-1) that contributes to the growth of Listeria monocytogenes in suboptimal conditions. J. Appl. Microbiol. 109 (3), 984–995.
Smith, A.M., Tau, N.P., Smouse, S.L., Allam, M., Ismail, A., Ramalwa, N.R., Thomas, J., 2019. Outbreak of Listeria monocytogenes in South Africa, 2017–2018: laboratory activities and experiences associated with whole-genome sequencing analysis of isolates. Foodborne Pathogen. Dis. 16 (7), 524–530.
Sprouffske, K., Wagner, A., 2016. Growthcurver: an R package for obtaining interpretable metrics from microbial growth curves. BMC Bioinf. 17 (1), 172.
Sumrall, E.T., Shen, Y., Keller, A.P., Rismondo, J., Pavlou, M., Eugster, M.R., Kilcher, S., 2019. Phage resistance at the cost of virulence: Listeria monocytogenes serovar 4b requires galactosylated teichoic acids for InlB-mediated invasion. PLoS Pathog. 15 (10), e1008032.
Suo, Y., Huang, Y., Liu, Y., Shi, C., Shi, X., 2012. The expression of superoxide dismutase (SOD) and a putative ABC transporter permease is inversely correlated during biofilm formation in Listeria monocytogenes 4b G. PloS One 7 (10).
To, T.-H., Jung, M., Lycett, S., Gascuel, O., 2016. Fast dating using least-squares criteria and algorithms. Syst. Biol. 65 (1), 82–97.
Todd, E., Notermans, S., 2011. Surveillance of listeriosis and its causative pathogen, Listeria monocytogenes. Food Contr. 22 (9), 1484–1490.
Wang, J., Ray, A.J., Hammons, S.R., Oliver, H.F., 2015. Persistent and transient Listeria monocytogenes strains from retail deli environments vary in their ability to adhere and form biofilms and rarely have inlA premature stop codons. Foodborne Pathogen. Dis. 12 (2), 151–158.
Ye, J., Coulouris, G., Zaretskaya, I., Cutcutache, I., Rozen, S., Madden, T.L., 2012. Primer-BLAST: a tool to design target-specific primers for polymerase chain reaction. BMC Bioinf. 13 (1), 134.